ELSEVIER

International Journal of Mass Spectrometry 177 (1998) 143–154

International Journal of Mass Spectrometry

Kinetic energies of ions produced by dissociative electron impact ionization of propane

H.U. Poll[1], V. Grill, S. Matt, N. Abramzon[2], K. Becker[2], P. Scheier, T.D. Märk*

Institut für Ionenphysik, Leopold-Franzens Universität, Technikerstrasse 25, A-6020 Innsbruck, Austria

Received 14 October 1997; accepted 8 April 1998

Abstract

Mass spectrometric techniques in conjunction with the ion deflection method have been used to measure kinetic energy spectra of the various ions produced by electron-impact ionization and dissociative ionization of propane, C_3H_8. The kinetic energy spectra of the $C_3H_i^+$ ions ($i = 0$–8) indicate that these ions are almost exclusively formed with quasithermal energies and that the mechanism of their formation is dominated by the removal of one or more neutral H and H_2 fragments accompanied in some cases by a molecular rearrangement of the residual fragment ion. The spectra of the $C_2H_i^+$ fragment ions ($i = 0$–5) show, besides a quasithermal peak, also ions with higher kinetic energies indicating that a fraction of the ions are the result of processes favoring the formation of energetic, nonthermal fragment ions. Although the quasithermal contribution is dominant in the spectra of the $C_2H_5^+$ and $C_2H_4^+$ fragment ions, the spectra of the smaller $C_2H_i^+$ ions ($i = 0$–3) show a dominance of energetic, nonthermal ions whose formation most likely proceeds via the initial excitation of high-lying repulsive target states. The spectra of the CH_i^+ fragment ions ($i = 1$–3) are dominated by the presence of energetic, nonthermal ions with kinetic energies of up to 4 eV per fragment ion with quasithermal ions accounting for only about 15% or less of the total ion signal. (Int J Mass Spectrom 177 (1998) 143–154) © 1998 Elsevier Science B.V.

Keywords: Electron ionization; Fragment ions; Propane; Kinetic energy

1. Introduction

The formation of ions by electron-impact ionization and dissociative ionization of molecules is an important process in many applications such as discharges and low-temperature plasmas, excimer lasers, radiation chemistry, fusion edge plasmas, radiation chemistry, mass spectrometry, and chemical analysis [1–5]. In many instances, the kinetic energy distribution of the fragment ions, in particular the presence of energetic fragment ions with kinetic energies of several electronvolts, can have a profound impact on the energy deposition and on the energy transfer and thus on the physical and chemical processes in these environments. Hydrocarbons are major constituents of many planetary atmospheres and they are important compounds in combustible gas mixtures and in fusion edge plasmas [1–5]. Propane, C_3H_8, is a prototypical linear hydrocarbon molecule whose ionization properties have been investigated before [6, 7]. Absolute total [8] and partial [9] electron impact cross sections for the formation of parent and fragment ions have

*Corresponding author.

[1]Permanent address: Sektion Physik, Technische Universität, Chemnitz, Germany.

[2]Dept. of Physics and Engineering Physics, Stevens Institute of Technology, Hoboken, NJ 07030.

PII S1387-3806(98)14035-6

been obtained and some information on the kinetic energy of fragment ions is available [9–13]. The determination of fragment ion kinetic energies is also interesting from a more basic viewpoint. It can provide information about the distribution of the collision energy among the various internal degrees of freedom of a molecule and about the high-lying repulsive electronic states of the molecule. In this context it is important to mention that mass spectra and breakdown graphs of propane (produced by electron impact ionization, photoionization and photoelectron coincidence methods) have been used many times as a quantitative test for the verification of the quasiequilibrium theory (QET) [14,15]. Moreover, there exist several studies concerning the metastable decay of propane and propane fragment ions with emphasis upon the relationship between metastable peak shapes, ion structure, and fragmentation mechanisms [16].

This article presents a comprehensive account about the kinetic energies of the various ions produced by electron-impact ionization and dissociative ionization of propane in the Nier-type ion source of a two-sector field mass spectrometer. Kinetic energy spectra were obtained and analyzed using a combination of mass spectrometric techniques and the ion deflection method [17] (this method and also other methods to measure the kinetic energies of ion fragments have been summarized and discussed in [10, 11,13,18]). Special care was exercised to ensure that ion discrimination effects, which affect the extraction, transport, and detection of fragment ions formed with different kinetic energies, were taken into account quantitatively. While the earlier paper by Grill et al. [9] reported already fragment ion kinetic energies for several fragment ions as did the papers of Fuchs and Taubert [10], the results presented in this article were obtained using a more detailed data analysis procedure. This resulted in revised values for the kinetic energies for most ions. In particular, we provide a more detailed analysis of the formation of energetic, nonthermal fragment ions than in the work of Grill et al. [9]. It is interesting to point out that (i) in contrast to the study of the kinetic energy release for metastable decay reactions for which there is a well-defined lifetime window (and therefore a well-defined corresponding internal energy window) and (ii) in contrast to coincidence experiments such as PEPICO or TPEPICO for which the internal energy is again well-defined, in the present measurements the decaying ions in the ion source producing the fragment ions probed correspond to a wide range of internal energies (and thus lifetimes up to approximately 1 μs).

2. Apparatus and experimental procedure

We used a combination of mass spectrometric techniques and the ion deflection method [17]. A detailed description of the high-resolution, double focusing sector field mass spectrometer, its performance and operating characteristics have been given in previous publications [9,13,17]. Furthermore, the principle of the ion deflection method has also been discussed recently in connection with the determination of the kinetic energies of fullerene fragment ions in our apparatus [19].

Briefly, we use a double focusing Nier–Johnson two-sector field mass spectrometer of reversed geometry with a Nier-type electron-impact ion source. The target gas beam is crossed by a well-characterized magnetically collimated electron beam (electron beam energy usually 100 eV, FWHM energy spread about 0.5 eV). The product ions are extracted from the ion source by a penetrating electric field, accelerated to about 3 kV and subsequently pass a pair of mutually perpendicular deflection plates which allow us to sweep the product ion beam across the entrance slit of the first field region in two directions in order to determine vertical and horizontal profiles of the ion beam for each product ion. After passing through a magnetic sector field for momentum analysis, the ions enter a second field-free region followed by an electric sector field which acts as an energy analyzer. The mass- and energy-selected ions are further accelerated before they are detected by a channel electron multiplier operated in the pulse counting mode.

A schematic diagram of the elements of the apparatus pertaining to the present studies is shown in Fig. 1. Ion beam profiles for each ion were obtained in the

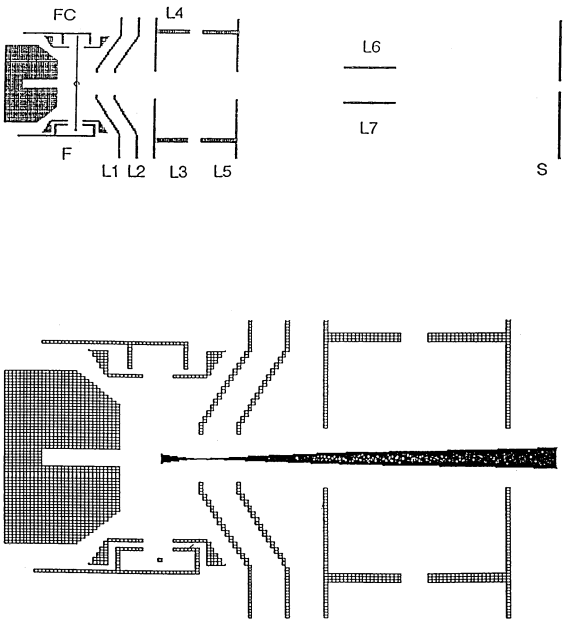

Fig. 1. Schematic view of the Nier-type ion source [17] showing in the upper part the electron beam between the filament (F) and Faraday cup (FC) and in the lower part the calculated ion trajectories after interaction of this electron beam with a perpendicular gas target beam (indicated in the upper part by a circle). L1 ion source exit electrodes, L2 ion extraction electrodes (penetrating field extraction, see [17]), L3, L4 focusing and steering electrodes, L5 earth slit, L6, L7, *z*-deflection plates and S mass spectrometer entrace slit.

z-direction by sweeping the ion beam across the entrance slit of the mass spectrometer using the deflection plates L_6 and L_7 and by recording the ion beam intensity as a function of the deflection voltage. In principle, two independent data analysis procedures can be applied to extract information about the kinetic energy distribution of the ion under study from the measured ion beam profiles as discussed in detail before in the context of our fullerene fragment ion investigation [19]. One method extracts the kinetic energy from the half-width of the ion profile (half-width method), whereas the other method analyzes the entire beam profile (profile method). In the present case, where the measured profiles are sometimes complex convolutions of quasithermal and energetic, nonthermal ion components, the full profiles were measured and analyzed for all ions under study.

A straightforward application of the ion deflection method yields a direct proportionality between the square of the deflection voltage in the *z* direction and the kinetic energy of the ions in the laboratory system (see also [11,13,18]). The kinetic energy of a given fragment ion consists of the initial thermal energy of the neutral propane molecule in the ion source (which is usually identical to the temperature of the neutral gas emanating from the gas nozzle) and any kinetic energy imparted to the fragment ion under study by the dissociative ionization process. Accordingly, even the $C_3H_8^+$ parent ions will show an energy distribution of finite width which reflects the thermal kinetic energy distribution of the neutral C_3H_8 molecules in the ion source (assuming that the electron-impact ionization process itself imparts only a negligible amount of kinetic energy on to the parent ion). In addition the width of the parent ion (and also of the fragment ions) could be broadened considerably by the ion extraction itself, if for instance the ions are starting from positions in the ion source with different extraction potentials. For smaller fragment ions, which can be the result of different fragmentation pathways, the kinetic energy also depends on the particular break-up mechanism, e.g. single-step, two-fragment break-up or sequential decay via several intermediate steps or a combination thereof. The proportionality constant between the measured ion intensity and the square of the deflection voltage can either be determined empirically by normalization to ions of known kinetic energy or it can be calculated for the specific experimental arrangement used [10]. For the present setup this constant has been previously determined to be 10^{-3} [9,13].

We illustrate the steps involved in the data acquisition and analysis procedure in the present case, where the measured ion beam profiles can be a complex convolution of several components, for the case of the measured CH_3^+ fragment ion profile [Figs. 2(a)–2(d)]. Fig. 2(a) shows the raw data, i.e. the measured ion signal $I(U_z)$ as a function of the deflection voltage U_z in the *z* direction. We then take the derivative of the ion signal after smoothing the original data set, if necessary [Fig. 2(b)]. A plot of this function vs. the square of the deflection voltage yields

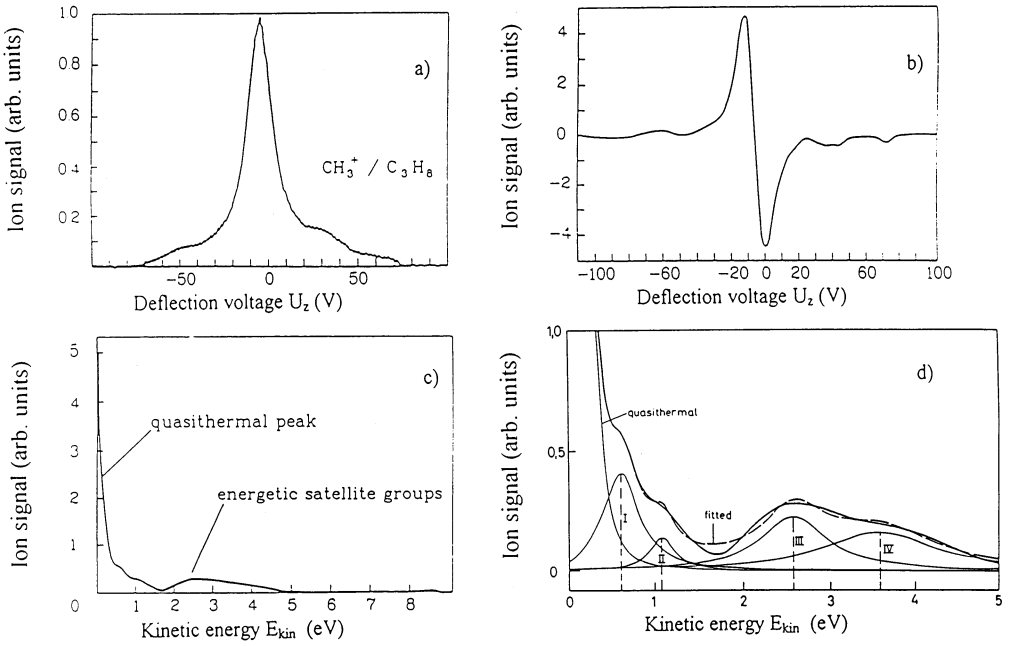

Fig. 2. Data acquisition and analysis steps in the present study: (a) Ion signal vs. deflection voltage U_z applied to the deflection plates L6, L7 in Fig. 1 (z-deflection curve [10,17]) for CH_3^+ fragment ions produced by electron ionization of propane; (b) ion signal given in (a) smoothed and differentiated; (c) kinetic energy distribution (ion signal vs. kinetic energy) obtained from (b) by proper normalization and calibration (see text) and (d) close up of energy distribution showing a possible fit (see text) to the data giving besides the quasithermal peak at very low energies in addition four ion components with larger kinetic energies.

the kinetic energy distribution $T(E_{kin})$ shown in Fig. 2(c) after proper normalization

$$\int_0^\infty T(E_{kin})\, dE_{kin} = 1 \qquad (1)$$

The above relation assumes that ions of different kinetic energies contribute equally to the measured ion signal. However, this is generally not the case. It is well known [2,20] that all mass spectrometers detect energetic fragment ions with significant discrimination. For the present apparatus, the discrimination has been quantified [9,13,17] and can be expressed in terms of an energy-dependent discrimination factor (or alternatively by an extraction efficiency) which is shown in Fig. 3. It is obvious from Fig. 3 that all energetic fragment ions are detected with a much reduced detection efficiency and that even thermal parent ions are detected with an efficiency of less than 100% (it is interesting to note that by using a different extraction method at least for thermal parent ions 100% extraction efficiency can be achieved [21]). Therefore, the energy distribution of Fig. 2(c) obtained from the measured ion profile has

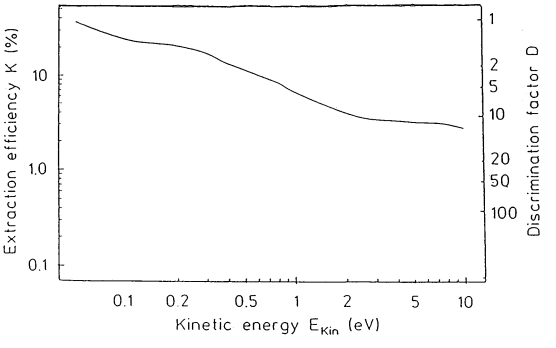

Fig. 3. Extraction efficiency (left hand scale) and discrimination factor D (right hand scale) vs. kinetic energy of the ion for ions (produced in the Nier-type ion source shown schematically in Fig. 1) after Grill et al. [9].

to be corrected using the discrimination factor displayed in Fig. 3 in order to obtain the true kinetic energy distribution $f(E)$. Alternatively, the correction can also be applied directly to the measured ion beam profile of Fig. 2(a) prior to any data reduction or (and this has been done in the present article) to the various apparent ion components extracted in the final step of the data analysis. This final step in the data analysis is the extraction of the various ion components contained in the spectrum corresponding to different kinetic energies from the energy distribution of Fig. 2(c). This is done by fitting the entire spectrum to a series of individual distributions using either a Gauss or a Lorentz profile for each distribution. Integration over the individual peak areas and multiplication with the corresponding discrimination factor yields the true contribution to the total kinetic energy distribution for that particular fragment ion. Common to the energy spectra recorded for most fragment ions were two distinct energy regimes, one corresponding to the formation of thermal and quasithermal ions and a broad distribution corresponding to the formation of energetic fragment ions.

The quasithermal peak may be represented by a thermal distribution function $f(E)$ of the form [10]

$$f(E) = H(E/E_0)^{1/2} \exp[(E_0 - E)/2E_0] \quad (2)$$

where E represents the kinetic energy of the ions. Then, the distribution function $f(E)$ has its maximum at $E = E_0 = 1/2kT$ (k refers to the Boltzmann constant and T denotes the absolute temperature) and H is the maximum value of the distribution function, $H = f_{max} = f(E_0)$. The average thermal energy E_{th} is given by $E_{th} = 3E_0 = 3/2kT$. E_{th} is also related to two other quantities that can be obtained from the energy distribution of Eq. (2) above, the half-width energy $E_{1/2}$ given by $E_{1/2} = 1.23E_{th}$ and the half-width E_{HW} of the integrated distribution $\int f(E)\,dE$ given by $E_{HW} = 1.11E_{th}$ [10].

Fig. 2(d) shows an enlarged part of the energy distribution of Fig. 2(c), which highlights the regime of higher kinetic energies. Fig. 2(d) also illustrates the challenge of interpreting and representing a complex energy distribution by a series of individual profiles.

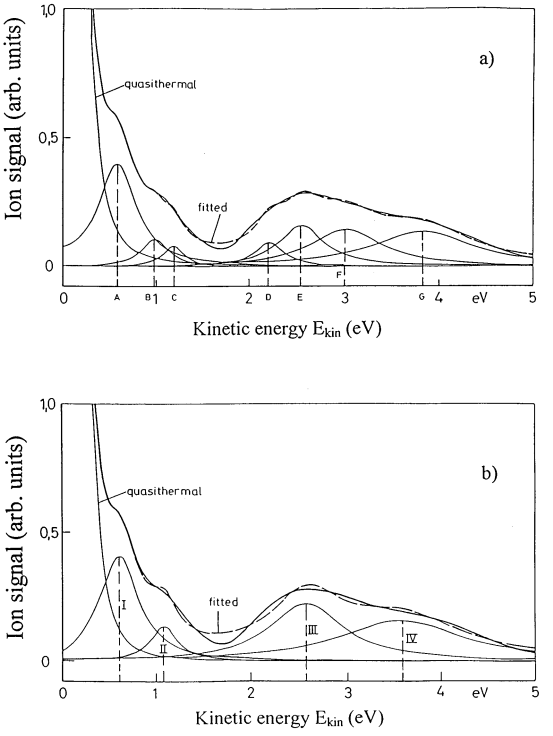

Fig. 4. Kinetic energy distribution (ion signal vs. kinetic energy) in the quasithermal regime for CH_3^+ fragment ions produced by electron ionization of propane. The data can be fitted with different numbers of individual peaks (see text), i.e. 6 individual peaks in (a) and 4 individual peaks in (b). For details see text.

As shown in Figs. 4(a) and 4(b), the fitting procedure does not lead to unique and unambiguous results and it could as well be argued that the energy distribution only consists of one quasithermal and one broad higher energy component (the various quasipeaks being due to experimental artefacts). Fig. 4(a), for example, shows a fit of the CH_3^+ fragment ion energy distribution using 6 individual peaks, whereas Fig. 4(b) shows the same CH_3^+ energy distribution represented by 4 individual peaks. Independent of the question of the true energy distribution (it is conceivable that the measured distribution also suffers from broadening due to space charge and other effects in the ion source, during the extraction and deflection; measurements with a higher energy resolution than available in the present case would be highly desirable) this fitting procedure facilitates the correction

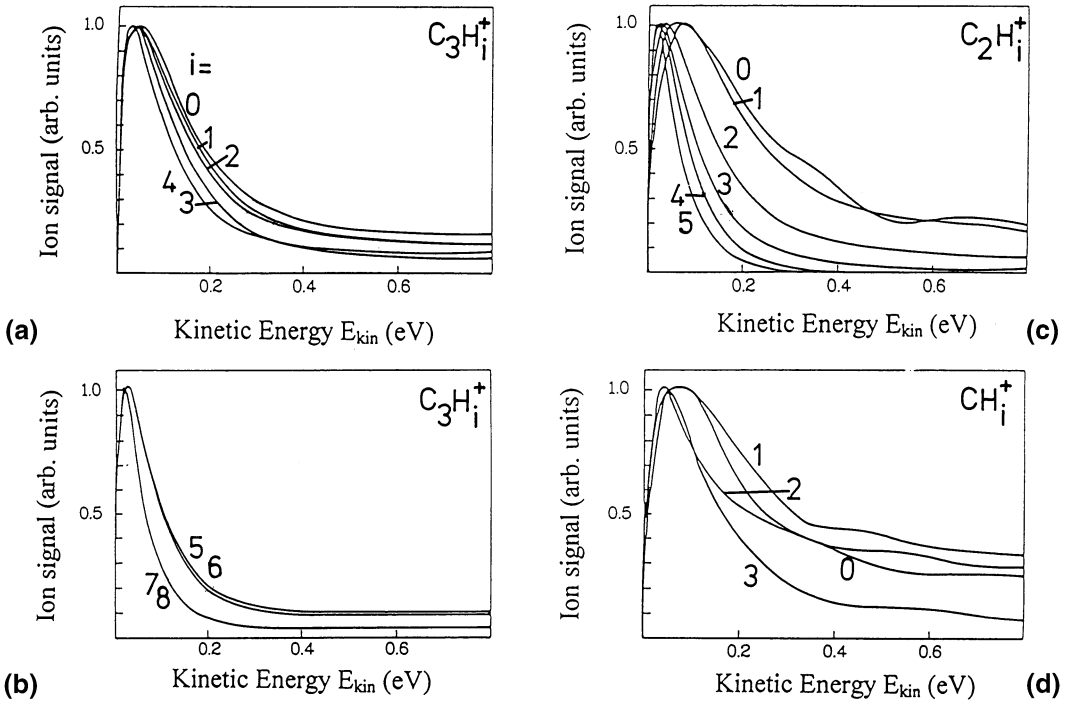

Fig. 5. Kinetic energy distribution (ion signal vs. kinetic energy) in the quasithermal regime for $C_3H_i^+$, $C_2H_i^+$, and CH_i^+ produced by electron ionization of propane.

procedure outlined above in order to account for energy-dependent discrimination.

3. Results and discussion

Most fragment ion kinetic energy spectra recorded here show two separate features, a pronounced peak at low kinetic energies ($E < 0.5$ eV) which corresponds to the formation of thermal and near-thermal fragment ions and a broad energy distribution extending to several electronvolts which represents the formation of energetic nonthermal fragment ions. The two regions of the energy spectra will be discussed separately in the following sections.

3.1. The formation of quasithermal ions

Fig. 5 shows an enlargement of the quasithermal part of the kinetic energy spectra for various fragment ions. Figs. 5(a) and 5(b) show the spectra of the $C_3H_i^+$ fragment ions for $i = 0$–4 [Fig. 5(a)] and $i = 5$–8 [Fig. 5(b)]. It is apparent from Fig. 5(b) that the energy distributions of, respectively, the $C_3H_8^+$ parent ions and the $C_3H_7^+$ fragment ions are essentially identical with average thermal energies of $E_{th} = 0.049$ eV ($C_3H_8^+$) and $E_{th} = 0.050$ eV ($C_3H_7^+$). The value of 0.049 eV for the $C_3H_8^+$ parent ion corresponds to a "gas temperature" of about 380 K, which is slightly higher than the room temperature because of the additional effects discussed above. As expected, the energy distribution becomes increasingly broader for smaller fragment ions and the maximum in the distribution function is shifted to higher energies. Table 1 summarizes the average thermal energies E_{th} for the $C_3H_i^+$ ions obtained from the present analysis and compares the results with the earlier values reported by Grill et al. [9] and with the values from Fuchs and Taubert [10].

Figs. 5(c) and 5(d) show the quasithermal energy

Table 1
Experimentally determined values of the thermal energies E_{th} (see text) and E_{HW} (see text) of the $C_3H_i^+$ ions (i = 0–8) produced by electron-impact ionization and dissociative ionization of C_3H_8

Ion	E_{th} (eV), this work	E_{HW} (eV), [9]	E_{th} (eV), [10]
$C_3H_8^+$	0.049	0.04	0.056
$C_3H_7^+$	0.050	0.06	0.059
$C_3H_6^+$	0.074	0.09	0.083
$C_3H_5^+$	0.073	0.09	0.092
$C_3H_4^+$	0.091	0.08	0.13
$C_3H_3^+$	0.112	0.08	0.17
$C_3H_2^+$	0.126	0.14	0.20
C_3H^+	0.135	0.14	0.21
C_3^+	0.145	0.12	0.22

distributions for, respectively, the $C_2H_i^+$ (i = 0–5) and the CH_i^+ (i = 0–3) fragment ions. The $C_2H_i^+$ energy distributions show a behavior which is in many qualitative aspects similar to that of the $C_3H_i^+$ distributions before, viz. the distribution becomes increasingly broader with a maximum at higher energies for smaller fragment ions. There is one noteworthy exception, the distribution for the $C_2H_4^+$ fragment ions lies below the distribution of the $C_2H_5^+$ fragment ions, i.e., the smaller $C_2H_4^+$ ions are formed with less kinetic energy than the larger $C_2H_5^+$ ions. This finding is similar to what was observed earlier by Fuchs and Taubert for these two fragment ions [10]. This finding is in accordance with earlier observations which indicate that at least at threshold $C_2H_4^+$ is formed by ejection of a CH_4 unit and is no product of a H loss from the $C_2H_5^+$ ion. Furthermore, the kinetic energies are as expected from the respective breakdown curves, i.e. the breakdown curve for $C_2H_4^+$ is very narrow, whereas that for $C_2H_5^+$ formation which occurs by a loose transition state covers a wide internal energy range. We also note that in the case of the formation of the bare C_2^+ fragment ion [i = 0 in Fig. 5(c)] there is no longer a clear distinction between the quasithermal part of the energy distribution and the high-energy, nonthermal part. This partial overlap is even more pronounced in the case of the formation of the CH_i fragment ions (i = 0–3) shown in Fig. 5(d) and complicates the data analysis in terms of individual ion components for these fragment ions.

Table 2
Experimentally determined values of the thermal energies of the $C_2H_i^+$ ions (i = 0–5) produced by electron-impact dissociative ionization of C_3H_8

Ion	E_{th} (eV), this work	E_{HW} (eV), [9]	E_{th} (eV), [10]
$C_2H_5^+$	0.069	0.08	0.079
$C_2H_4^+$	0.052	0.06	0.069
$C_2H_3^+$	0.081	0.08	0.16
$C_2H_2^+$	0.115	0.10	0.32
C_2H^+	0.213	0.28	0.38
C_2^+	0.213	0.18	0.52

The present results for the average thermal energies E_{th} for these quasithermal energy distributions of the various $C_2H_i^+$ fragment ions are summarized in Table 2 in comparison with the earlier results of Grill et al. [9] and Fuchs and Taubert [10]. Table 3 lists the present average thermal energies for the CH_i^+ fragment ions which are compared to the previous results of Grill et al. [9]. No other experimental data are available for these fragment ions.

A comparison of the present results for the $C_3H_i^+$ fragment ions with the other available data shows that there is overall satisfactory agreement with the data obtained from the earlier analysis by Grill et al. [9] (perhaps with the exception of the $C_3H_3^+$ and C_3^+ ions), but that there are some significant discrepancies with the data reported by Fuchs and Taubert [10], particularly for the lighter fragment ions, where our analysis systematically yields lower values of the quasithermal energy. A similar observation can be made for the $C_2H_i^+$ data shown in Table 2. Again, there is good agreement with the earlier analysis of Grill et al. [9] (except for the C_2H^+ ion), whereas the

Table 3
Experimentally determined values of the thermal energies of the CH_i^+ ions (i = 0–3) produced by electron-impact dissociative ionization of C_3H_8

Ion	E_{th} (eV), this work	E_{HW} (eV), [9]
CH_3^+	0.112	0.28
CH_2^+	0.120	0.31
CH^+	0.204	0.67
C^+	0.193	0.37

energies reported by Fuchs and Taubert [10] are increasingly larger than our energies as the fragment ions get smaller. For the C_2^+ fragment ion, for instance, our energy is less than half the energy reported by Fuchs and Taubert [10]. In contrast, there is rather poor agreement between the energies determined in this work and the energies from the earlier analysis of Grill et al. [9] for the CH_i^+ fragment ions. Our energies are systematically smaller by as much as a factor of 3 (for the CH^+ ion).

The quasithermal kinetic energies for the various fragment ions in Tables 1–3 show that all but the largest fragment ions are formed with kinetic energies that are larger, in some cases much larger than what can be attributed to the temperature of the target molecule in the ion source. For all fragment ions formed via a dissociative ionization process, the measured quasithermal kinetic energy consists of a contribution from the thermal motion of the propane gas molecules in the interaction region and a certain excess kinetic energy imparted on the ionic fragment as a result of the break-up of the target into two (or more) fragments. The "thermal" component (including broadening due to additional effects in the ion source and during the ion extraction) can be obtained from the kinetic energy measured for the $C_3H_8^+$ parent ions. In our case, we find a value of 0.049 eV corresponding to a "gas temperature" of 380 K, somewhat more than the room temperature, which is not an unrealistic value for an ion source operating at optimum conditions. The excess kinetic energy, on the other hand, has its origin in the energy that is transferred to the target in the electron collision process and that is subsequently distributed among the dissociating fragments in some fashion that depends on the exact mechanism and dynamics of the breakup. Because we only detect one fragment ion in our experiment, it is impossible to uniquely identify the breakup mechanism that leads to the formation of a particular fragment ion. The quantities that are determined experimentally, such as the kinetic energy of the fragment ion under study and its appearance energy, in conjunction with some assumptions about the breakup mechanism based on experience and empirical results with the fragmentation of other molecules, can help narrow down the possible breakup mechanisms and identify the most probable pathways leading to the formation of a particular fragment ion, particularly in the case of the larger fragment ions where there are fewer possible decomposition routes.

One model, the quasiequilibrium theory (QET) [15,22], assumes that the collision energy imparted to the target is initially distributed statistically among the various electronic, vibrational, and rotational excitations until an equilibrium is reached. The statistical fluctuations of the energy can lead to an accumulation of energy in a particular chemical bond which is sufficiently large to break that bond. Depending on the particular transition state kinetic energy (called total kinetic energy release, KER) is then carried away by the dissociating fragments and is distributed among the fragments in accordance with momentum conservation. In the case of a two-fragment breakup of the $C_3H_8^+$ parent ion into a particular fragment ion and a ground-state neutral, one finds the following relationship:

$$E_{\mathrm{CM}} = E_{\mathrm{th,fr}}(M/m_n) - E_{\mathrm{th,pa}}(m/m_n) \tag{3}$$

between the center-of-mass KER energy E_{CM}, the kinetic energy of the fragment ion $E_{\mathrm{th,fr}}$, and the thermal energy of the parent ion in the laboratory frame $E_{\mathrm{th,pa}}$. M, m, and m_n denote the mass of, respectively, the parent ion, the fragment ion, and the ground-state neutral. A derivation and detailed discussion of the well-established Eq. (3) can be found in the paper of Muigg et al. [19] and in references cited therein. Eq. (3) leads to a linear relationship between the measured kinetic energy of the fragment ion and the mass of the fragment ion m, i.e.

$$E_{\mathrm{th,fr}} = E_{\mathrm{CM}} - (E_{\mathrm{CM}} - E_{\mathrm{th,pa}})m/M \tag{4}$$

This dependence is shown to hold approximately for the $C_3H_i^+$ fragment ions in Fig. 6 where we plotted the measured kinetic energy of the $C_3H_i^+$ fragment ions against their atomic mass number and thus indicates immediately, that E_{CM} is about constant and independent from the fragment size produced. The straight line might suggest that there is only a single fragmen-

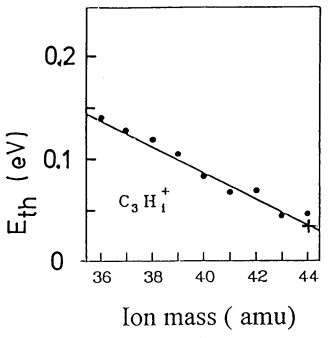

Fig. 6. Average thermal energy E_{th} vs. ion mass for $C_3H_i^+$ ions (i between 8 and 0) produced by electron ionization of propane.

tation sequence, viz. the successive removal of H atoms according to

$$\begin{array}{lcccc} C_3H_8^+ \rightarrow & C_3H_7^+ & + & H & \\ & \downarrow & & & \\ & C_3H_6^+ & + & H & \\ & \downarrow & & & \\ & C_3H_5^+ & + & H & \end{array} \qquad (5)$$

The analysis of Fig. 6 leads to a center-of-mass energy of $E_{CM} = 0.62$ eV for a thermal energy of $E_{th} = 0.049$ eV of the $C_3H_8^+$ parent ion in the first step of this fragmentation sequence. As a consequence, each H atom would on average carry away an excess energy of 0.57 eV. This at least is not true for the first step where the individual data points are approximately equal and where it is known that H loss from $C_3H_8^+$ again has a very small breakdown curve. In the case of the formation of the C_3^+ fragment ion where all 8 H atoms are removed, this would mean that almost 5 eV of kinetic energy alone have to be stored in the parent ion initially. One would have to add to this the energy required to break one or more of the C–H bonds. Although the removal of a neutral ground-state H atom is the likely channel leading to the formation of the $C_3H_7^+$ fragment ion, the formation of the lighter $C_3H_i^+$ fragment ions ($i = 0$–6) is unlikely to proceed via sequential H removal because of the significant amount of energy that would have to be transferred to the target in the initial collision process. The removal of one or more neutral H and H_2 fragments in conjunction with a molecular rearrangement of the residual fragment ion to lower its internal energy are more likely the main formation pathways leading to the lighter $C_3H_i^+$ fragment ions (in accordance with considerations by Fuchs and Taubert [10], this removal must occur in such a way that either the single fragments are ejected sequentially or in a single-step ejection mechanism—in the latter case the energy released is the smallest). This notion is supported by the observed appearance energies for the various $C_3H_i^+$ fragment ions that, in turn, are too low to render the sequential H removal a likely channel leading to the formation of the lighter $C_3H_i^+$ fragment ions [10].

If we apply the above analysis for the $C_3H_i^+$ fragment ions (Fig. 6) to the $C_2H_i^+$ and CH_i^+ fragment ions, we do not find a similar linear relationship. Although it is conceivable that the $C_2H_5^+$ and CH_3^+ fragment ions are the result of the single-step removal of, respectively, a neutral CH_3 or C_2H_5 radical, the lighter ions along the $C_2H_i^+$ and CH_i^+ fragment ion sequence are more likely the result of more complex fragmentation channels including processes in which a high-lying repulsive target state is excited in the initial electron collision (see discussion below and a detailed discussion of posssible fragmentation routes in [10]).

3.2. The formation of energetic, nonthermal fragment ions

The analysis of the energetic, nonthermal parts of the kinetic energy spectra of the various fragment ions reveals common trends, which are particularly pronounced for the light fragment ions CH_i^+ and $C_2H_i^+$ and which cannot be inferred from the previously discussed fragmentation channels leading to the formation of the quasithermal fragment ions. The most detailed analysis can be performed for the case of the CH_i^+ fragment ions shown in Fig. 7. Table 4 summarizes the energies of the various nonthermal peak positions labeled “A” through “G” in the kinetic energy spectra of the four fragment ions CH_3^+, CH_2^+, CH^+, and C^+ together with the energy of the quasithermal fragment ions. For each ion, we also give the relative contribution of the quasithermal and the

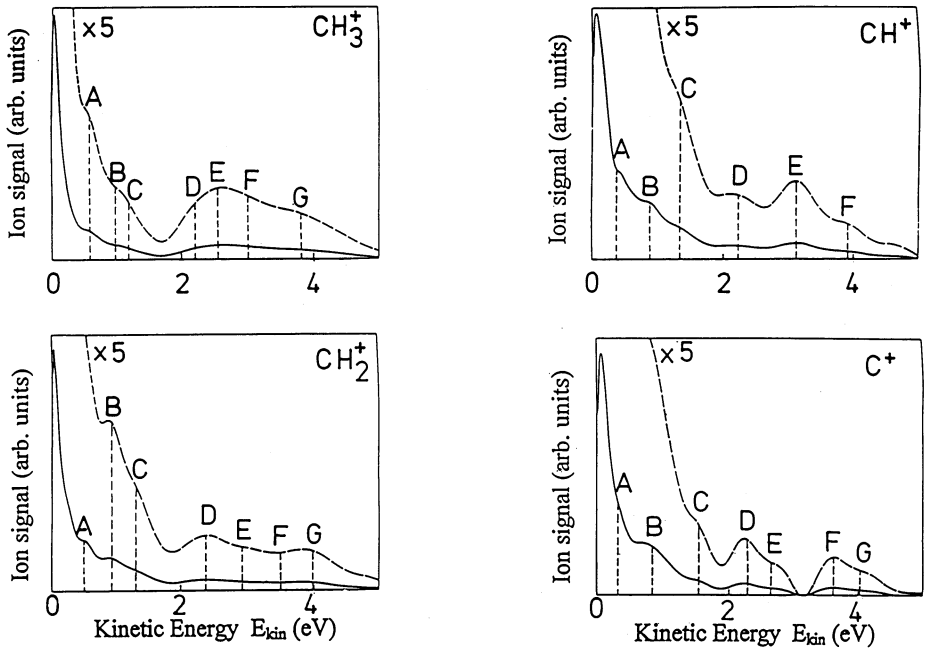

Fig. 7. Kinetic energy distribution (ion signal vs. kinetic energy) for CH_i ions produced by electron ionization of propane.

various nonthermal ion components to the total ion signal for that particular fragment ion after proper allowance for the discrimination (as given in Fig. 3) has been made. The following observations should be noted: (1) quasithermal fragment ions amount to only about 10% of all fragment ions produced, i.e., the formation of energetic, nonthermal ions is the dominant process for all four CH_i^+ fragment ions (i = 0–3), (2) for all hydrogen-bearing fragment ions a significant number (>25%) of very energetic ions with kinetic energies above 3 eV are produced. The mechanism by which the energetic, nonthermal frag-

Table 4
Kinetic energies of the CH_i^+ fragment ions (i = 0–3) produced by electron impact dissociative ionization of C_3H_8. Given are the thermal energy, the energy of several peak positions marked in Fig. 7 in the measured kinetic energy distributions corresponding to the formation of energetic, nonthermal ions, and the relative contribution of each ion group to the total signal recorded for that particular ion after proper correction for discrimination effects

	Energetic, nonthermal fragment ions								
	Quasithermal fragment ions								
	Thermal	A	B	C	D	E	F	G	Σ_{A-G}
Ion	E_{th} (eV) (%)	E_{kin} (eV) (%)	E_{kin} (eV) (%)	E_{kin} (eV) (%)	E_{kin} (eV) (%)	E_{kin} (eV) (%)	E_{kin} (eV) (%)	E_{kin} (eV) (%)	(%)
CH_3^+	0.112	0.59	0.99	1.19	2.21	2.55	3.01	3.82	
	5.6	13.0	3.9	2.6	5.8	15.4	22.7	31.0	94.4
CH_2^+	0.120	0.50	0.93	1.30	2.38	2.93	3.50	3.99	
	5.4	16.1	16.6	12.4	16.3	5.6	12.0	15.6	94.6
CH^+	0.204	0.38	0.89	1.34	2.22	3.12	3.92	—	
	8.2	25.0	16.2	14.2	7.4	23.7	5.3	—	91.8
C^+	0.193	0.31	0.83	1.53	2.27	2.64	3.61	4.02	
	14.6	14.7	44.0	1.6	8.1	2.9	6.5	7.6	85.4

Table 5
Kinetic energies of the $C_2H_i^+$ fragment ions (i = 0–5) produced by electron impact dissociative ionization of C_3H_8. Given are the thermal energy, the energy of several peak positions marked in Fig. 7 in the measured kinetic energy distributions corresponding to the formation of energetic, nonthermal ions, and the relative contribution of each ion group to the total signal recorded for that particular ion after proper correction for discrimination effects

	Energetic, nonthermal fragment ions						
	Quasithermal fragment ions						
	Thermal	A	B	C	D	E	Σ_{A-G}
	E_{th} (eV)	E_{kin} (eV)	E_{kin} (eV)	E_{kin} (eV)	E_{kin} (eV)	E_{kin} (eV)	
Ion	(%)	(%)	(%)	(%)	(%)	(%)	(%)
$C_2H_5^+$	0.069	0.71	—	1.61	2.69	—	
	87.9	11.5	—	0.1	0.5	—	12.1
$C_2H_4^+$	0.052	0.74	0.95	1.58	2.17	2.78	
	68.7	7.7	7.6	10.8	1.7	3.5	31.3
$C_2H_3^+$	0.081	0.72	—	1.74	2.38	—	
	36.8	51.6	—	6.3	5.3	—	63.2
$C_2H_2^+$	0.115	0.69	—	—	2.14	—	
	26.1	70.1	—	—	3.8	—	73.9
C_2H^+	0.213	0.68	1.05	1.50	2.47	—	
	26.0	29.8	24.9	16.3	3.0	—	74.0
C_2^+	0.213	0.72	1.06	1.69	2.67	—	
	16.9	25.0	32.3	16.8	9.0	—	83.1

ment ions are formed is not entirely clear. It is unlikely that they are formed in a process that can be described using the previous QET model. It is more likely that they result from the breakup of the parent molecule that is initially excited to a high-lying repulsive state (see [6]). The high density of such states for complex polyatomic molecules and the comparatively poor electron energy resolution in our experiment make it impossible to identify the particular precursor state of a given fragment ion from, e.g. a determination of the appearance energy. Moreover, as argued by Erhardt and Tekaat [6] some of the fragment ions produced with high kinetic energy may also be the result of the decay of a doubly charged parent ion initially formed by the electron impact ionization, i.e. $C_3H_8^{2+} \rightarrow C_2H_5^+ + CH_3^+$.

A somewhat different picture was found for the kinetic energy spectra of the $C_2H_i^+$ fragment ions (i = 0–5). Table 5 summarizes the energy of the various nonthermal peak positions labeled "A" through "E" designated in the kinetic energy spectra of the six fragment ions $C_2H_5^+$, $C_2H_4^+$, $C_2H_3^+$, $C_2H_2^+$, C_2H^+, and C^+ together with the energy of the quasithermal fragment ions. For each ion, we also give the relative contribution of the quasithermal and the various nonthermal ion components to the total ion signal for that particular fragment ion after proper allowance for the discrimination (as given in Fig. 3) has been made. The following observations for the $C_2H_i^+$ fragment ions are noteworthy: (1) the relative contribution of the quasithermal ions decreases monotonically from the heavy $C_2H_5^+$ fragment ion (where it is the by far strongest ion signal with 88% of the total signal) to the light C_2H^+ and C_2^+ fragment ions (where it amounts to only 20% of the total ion signal); (2) in comparison with the CH_i^+ fragment ions there is only a very small fraction of very energetic $C_2H_i^+$ fragment ions with kinetic energies exceeding 2 eV.

The kinetic energy spectra of the $C_3H_i^+$ fragment ions (i = 0–7) and of the $C_3H_8^+$ parent ion did not reveal any discernible evidence of the presence of energetic, nonthermal ions. All ions that retain the C–C–C structure appear to be formed with essentially not much of an excess kinetic energy. This is not entirely unexpected given the fact that the fraction of energetic, nonthermal ions and the amount of excess kinetic energy was already significantly less for the $C_2H_i^+$ fragment ions (which retain a C–C structure) compared to the CH_i^+ fragment ions that only contain a single C atom.

Acknowledgements

This work has been carried out within the association EURATOM-ÖAW and was supported by the FWF, OENB, and BMWV, Wien, Austria and in part by the US National Aeronautics and Space Administration (NASA) through a grant from the Planetary Atmospheres Program. It is a pleasure to thank Professor Chava Lifshitz, Jerusalem, for valuable comments concerning the subject of this article.

References

[1] L.G. Christophorou (Ed.), Electron Molecule Interactions and their Applications, Academic, Orlando, 1984.
[2] T.D. Märk, G.H. Dunn, Electron Impact Ionization, Springer-Verlag, Wien, 1985.
[3] L.C. Pitchford, B.V. McKoy, A. Chutjian, S. Trajmar (Eds.), Swarm Studies and Inelastic Electron-Molecule Collisions, Springer, New York, 1987.
[4] L.H. Toburen, Y. Hatano, Z. Herman, T.D. Märk, S. Trajmar, J.J. Smith, IAEA-TEC DOC, 506 (1989) 23.
[5] R.K. Janev, Atomic and Molecular Processes in Fusion Edge Plasmas, Plenum, New York, 1995.
[6] H. Erhardt, T. Tekaat, Z. Naturforschg. 19a (1994) 1382.
[7] H.M. Rosenstock, K. Draxl, B.W. Steiner, J.T. Herron, J. Phys. Chem. Ref. Data 6 (1997) (Suppl 1).
[8] B.L. Schram, M.J. van der Wiel, F.J. de Heer, H.R. Moustafa, J. Chem. Phys. 44 (1966) 49; N. Djuric, I. Cadez, M. Kurepa, Int. J. Mass Spectrom. Ion Processes 108 (1991) R1.
[9] V. Grill, G. Walder, D. Margreiter, T. Rauth, H. U. Poll, P. Scheier, T.D. Märk, Z. Phys. D 25 (1993) 217.
[10] R. Taubert, Z. Naturforschg. 19a (1964) 484; R. Fuchs, R. Taubert, Z. Naturforschg. 19a (1964) 494; R. Taubert, Z. Naturforschg. 19a (1964) 911; R. Fuchs, R. Taubert, Z. Naturforschg. 19a (1964) 1181.
[11] D.K. Sen Sharma, J.L. Franklin, Int. J. Mass Spectrom. Ion Phys. 13 (1974) 139.
[12] A.I. Ossinger, E.R. Weiner, J. Chem. Phys. 65 (1976) 2892.
[13] H.U. Poll, C. Winkler, D. Margreiter, V. Grill, T.D. Märk, Int. J. Mass Spectrom. Ion Processes 112 (1992) 1.
[14] F.W. McLafferty, Mass Spectrometry of Organic Ions, Academic, New York, 1963.
[15] K. Levsen, Fundamental Aspects of Organic Mass Spectrometry, Verlag Chemie, Weinheim, 1978.
[16] J.L. Holmes, J.K. Terlouw, Org. Mass Spectrom. 15 (1980).
[17] K. Stephan, H. Helm, T.D. Märk, J. Chem. Phys. 73 (1980) 3763; D. Margreiter, G. Walder, H. Deutsch, H.U. Poll, C. Winkler, K. Stephan, T.D. Märk, Int. J. Mass Spectrom. Ion Processes 100 (1990) 143.
[18] R.G. Cooks, J.H. Beynon, R.M. Caprioli, G.R. Lester, Metastable Ions, Elsevier, Amsterdam, 1973.
[19] D. Muigg, P. Scheier, K. Becker, T.D. Märk, J. Chem. Phys. 108 (1998) 963.
[20] L.J. Kiefer, G.H. Dunn, Rev. Mod. Phys. 38 (1966) 1.
[21] R. Basner, M. Schmidt, H. Deutsch, V. Tarnovsky, A. Levin, K. Becker, J. Chem. Phys. 102 (1995) 770.
[22] C. Brunne, H. Voshage, Massenspektrometrie, Thiemig, München, 1964.